Paleobiology

www.cambridge.org/pab

Kungurian extinctions in eupelycosaurs: a press–pulse event?

Michel Laurin[1,2,3], Gilles Didier[4], Sylvain Richoz[5], Matteo Montagna[6] and Evelyn Kustatscher[7]

[1]Centre de recherche en paléontologie – Paris, UMR 7207, Muséum national d'histoire naturelle, 75005 Paris, France
[2]Sorbonne Université, 75005 Paris, France
[3]Centre national de la recherche scientifique, Paris, France
[4]Université de Montpellier, CNRS, 34090 Montpellier, France
[5]Department of Geology, Lund University, Lund, Sweden
[6]Department of Agricultural Sciences, University of Naples Federico II, Italy
[7]Department of Natural History, Tirolean State Museums, 6060 Hall in Tirol, Austria

Article

Cite this article: Laurin, M., G. Didier, S. Richoz, M. Montagna, and E. Kustatscher (2026). Kungurian extinctions in eupelycosaurs: a press–pulse event?. *Paleobiology* **52**, 373–387. https://doi.org/10.1017/pab.2026.10102

Received: 28 June 2025
Revised: 08 March 2026
Accepted: 13 April 2026

Handling Editor:
Cindy Looy

Corresponding author:
Michel Laurin;
Email: michel.laurin@mnhn.fr

Abstract

The fossil record offers a unique window into patterns of extinction and biodiversity recovery over deep time, and recent advances in analytical methods have significantly enhanced this research field. Our analysis of an updated dataset that includes 50 terminal taxa and 175 fossil occurrences of Ophiacodontidae, Edaphosauridae, and Sphenacodontidae (OES grade hereafter) using a recent implementation of the skyline fossilized birth–death model (FBD hereafter) confirms our previous conclusion that the OES grade diversified during the latter half of the Pennsylvanian but waned thereafter. However, our new results differ in several important points compared with our previous study (published in 2024). Notably, the transition between these two diversification regimes seems to have occurred earlier (at 298.9 Ma, at the Carboniferous/Permian transition), and it appears to have been marked by a moderate (0.527 survival probability), previously unreported extinction event. Also, the OES grade seems to have experienced a much more severe mass extinction event in the mid-Kungurian, with an estimated survival rate of only 0.113, which left very few surviving OES grade lineages. Climatic instability that started around the Carboniferous/Permian boundary and lasted throughout the Cisuralian, plausibly caused by intense volcanism of the Tarim Large Igneous Province and the Panjal Traps, may explain this pattern, which consists of a stagnating biodiversity followed by a brief, severe extinction event. This is reminiscent of the press–pulse model proposed by Arens and West in 2008, but if there was indeed an end-Carboniferous crisis, it could also be viewed as a new, more complex, pulse–press–pulse pattern.

Non-technical Summary

Fossils give us a rare look into how life on Earth has changed over hundreds of millions of years, showing when species appeared, thrived, and disappeared. Using recently developed mathematical modeling, we studied an updated dataset of three groups of early relatives of mammals: Ophiacodontidae, Edaphosauridae, and Sphenacodontidae. Our results confirm that these animals diversified during most of the late Carboniferous, but waned thereafter. However, our new results differ in several major points compared with our previous study (published in 2024). Notably, the slowdown in their diversification seems to have started earlier than we previously suggested, at the end of the Carboniferous, rather than early in the Permian, and it appears to have coincided with a moderate (53% survival probability), previously unreported extinction event. Moreover, this group seems to have experienced a much more severe crisis in the mid-Kungurian, which left very few surviving lineages. This pattern may be explained by a climate instability that started about 299 million years ago and lasted throughout the early Permian. This was likely caused by intense volcanism that produced large lava and volcanic ash deposits. The results seem to have been a stagnating biodiversity between two brief extinction events. This is reminiscent of the "press–pulse model," in which a prolonged buildup of stress (the press) is followed by a sudden, intense collapse (the pulse), but it differs by starting with a crisis. Thus, these early mammal relatives may have experienced a more complex series of events, consisting of two brief crises separated by a long period of stress.

© The Author(s), 2026. Published by Cambridge University Press on behalf of Paleontological Society. This is an Open Access article, distributed under the terms of the Creative Commons Attribution licence (http://creativecommons.org/licenses/by/4.0), which permits unrestricted re-use, distribution and reproduction, provided the original article is properly cited.

Introduction

The Permian (298.9–251.9 Ma) witnessed a spectacular diversification of amniotes and of other terrestrial life forms (Laurin 2010). The synapsids (mammal total group) dominated the terrestrial faunas until the end of the Permian, when the largest mass extinction event (i.e., the extinction of many lineages over a short period) took place (e.g., Irmis and Whiteside 2012;

Viglietti et al. 2021). After that crisis, reptiles would dominate the biosphere for the entire Mesozoic (Carroll 1988). However, important taxonomic turnover occurred in synapsids well before the end of the Permian. This may have result in part from an important climate change that occurred around the Carboniferous/Permian boundary. It consisted of global warming and aridification, as the Late Paleozoic Ice Age (LPIA) was waning (Montañez and Poulsen 2013; Richey et al. 2020). In addition, up to four mass extinction events have been recognized in the Permian alone (Lucas 2017; Didier and Laurin 2021). In chronological order, the first one is in the Sakmarian or the Artinskian (Benton 1985, 1989; Brocklehurst et al. 2013), between 293.5 and 283.3 Ma. The second, near the end of the Kungurian (Lucas 2017; Brocklehurst 2018), is often called "Olson's extinction" (Sahney and Benton 2008; Brocklehurst 2018, 2020), and occurred around 274.4 Ma. The third, near the end of the Capitanian (Day et al. 2015; Arefifard and Payne 2020; Rampino and Shen 2021; Fielding et al. 2023), is sometimes called the "dinocephalian extinction event" (Lucas 2009) and dates from 259.5 Ma. The famous end-Permian event (Ward et al. 2005; Smith et al. 2012; Viglietti et al. 2021), which was probably the most severe, occurred around 252 Ma. Recovery from that event may have extended into the Middle Triassic (Irmis and Whiteside 2012), possibly because other crises took place in the Early Triassic (Hochuli et al. 2016).

Of these four Permian mass extinction events, the one that resulted in the most spectacular faunal changes among synapsids is arguably the Kungurian event. It witnessed the demise of most lineages that originated during the first (Carboniferous and Cisuralian) evolutionary radiation of synapsids. These were ectothermic taxa (Faure-Brac and Cubo 2020; de Buffrénil et al. 2021) with a sprawling posture (Gônet et al. 2023) that bore little resemblance to mammals. These include five main clades, which we list in their order of inferred appearance, based on the established phylogeny (Reisz 1986; Huttenlocker et al. 2021). First, Caseasauria produced some fairly large herbivorous taxa. Second, varanopids included agile, typically midsized carnivores. Third, ophiacodontids were large predators and were long thought to have been amphibious. Fourth, the sail-backed edaphosaurids included the first known herbivorous amniotes. Fifth, the sphenacodontids, most of whom also had a sail, were the top predators on land (Romer and Price 1940; Reisz 1986). These synapsid taxa did not inhabit exactly the same habitats. Ophiacodontids, edaphosaurids, and to a lesser extent the sphenacodontids (collectively called "OES grade" hereafter) are believed to have inhabited lowlands (Romer and Price 1940; Olson 1975). This is shown in reconstructions of these animals in their presumed habitats (Fig. 1), although this does not necessarily imply that they spent much time swimming (Felice and Angielczyk 2014; Laurin and de Buffrénil 2016). Caseasauria and Varanopidae inhabited more upland environments (Brink et al. 2019), a little farther from large bodies of standing water.

A limited diversity of caseasaurs and varanopids extended well into the Guadalupian, after the Cisuralian. In contrast, ophiacodontids and edaphosaurids are unknown in the fossil record after the Kungurian, and the last sphenacodontid occurs barely later, in the early Roadian (Laurin and Hook 2022). Thus, by the Guadalupian, the synapsid faunas were dominated by the endothermic therapsids (Faure-Brac and Cubo 2020). These taxa had a more erect posture than earlier synapsids (Blob 2001), and are now represented by mammals (Sidor 2001; Angielczyk and Kammerer 2018). This brief taxonomic overview of early synapsids follows the established view that varanopids are synapsids. This long-established idea (Romer and Price 1940; Didier and Laurin 2024) has been challenged by a few (Laurin and Piñeiro 2018; MacDougall et al. 2018; Ford and Benson 2020), but not all (Benoit et al. 2021; Simões et al. 2022; Jenkins et al. 2024) recent studies.



Figure 1. Two typical lowland limbed vertebrates from the late Pennsylvanian and Cisuralian: *Ophiacodon mirus* holding a prey (an embolomere, an aquatic to amphibious stegocephalian) in its mouth. Reconstruction by Dmitry Bogdanov (a cardiologist and paleo-artist living in Chelyabinsk, Russia, who kindly gave us permission to reproduce it) sent to us by Amin Khaleghparast (a biologist from Tehran, Iran). Lower-resolution versions of this image are available in the Wikimedia commons at: https://commons.wikimedia.org/wiki/File:Ophiacodon_mirus.jpg.

Important gaps remain in our knowledge of how the ectothermic synapsids became extinct and how they were replaced by therapsids. Most notably, the fossil record of continental vertebrates is scant in the late Kungurian and early Roadian (Laurin and Hook 2022). That record is also geographically disjunct, being best represented by the U.S. Southwest (especially Texas, New Mexico, and Oklahoma) in the Kungurian (Olson 1962, 1967), and in the Russian Platform in the Roadian (Golubev 2015). A controversy surrounding the age of the youngest North American Permian lithological units that yielded continental vertebrates has existed since Olson's (1962, 1967) pioneering works, but it seems to have been settled recently (Lozovsky 2005; Brocklehurst 2020; Laurin and Hook 2022). Recent works (e.g., Forte et al. 2017; Spina et al. 2026) showed that most of the available paleobotanic evidence that had been used by Laurin and Hook (2022) is irrelevant to this issue, because it is compatible with a Kungurian or Roadian age (among others) of the San Angelo and Chickasha formations. However paleobotanical data formed only a minor part of the evidence provided by Laurin and Hook (2022). The early Roadian age advocated by that study was based primarily on vertebrate biostratigraphy and lithostratigraphy, in addition to marine fossils (fusulinids and ammonoids).

We undertook a series of studies to reassess the pattern of biodiversity evolution of early synapsids to better understand the demise of ectothermic synapsids (Didier and Laurin 2021, 2024). Our last study on the evolution of biodiversity of early synapsids found no evidence of mass extinction events in the OES grade, but we did find a strong drop in cladogenesis rate in the early Cisuralian. This suggested that the OES grade simply declined gradually and did not support a Kungurian mass extinction event (Didier and Laurin 2024). Our study on Varanopidae suggested that this clade became extinct in the Capitanian event, which is unsurprising, because the last varanopids occur only a little before the suspected extinction horizon (Laurin and Didier 2025). It also suggested a previously unrecognized extinction event near the Carboniferous/

https://doi.org/10.1017/pab.2026.10102 Published online by Cambridge University Press

Permian boundary. This is surprising, because according to Stanley and Yang (1994), that temporal interval featured few extinctions.

Here, we assess the dynamics of decline and extinction in three clades of eupelycosaurs: Ophiacodontidae, Edaphosauridae, and Sphenacodontidae. We also compare our results with our recent findings on varanopids (Laurin and Didier 2025). The fact that varanopids appear to have inhabited more upland environments (Brink et al. 2019) raises the possibility that differences in preferred habitat between these taxa might explain differences in their diversification dynamics.

Moreover, we compare our results with those that we previously obtained on the OES grade, using an earlier implementation of the fossilized birth–death model (FBD) (Didier and Laurin 2024) in which the limits between time slices had to be placed a priori rather than estimated. The current version of our software to assess the skyline FBD (introduced in Laurin and Didier 2025) estimates the age of the boundaries between time slices, in addition to estimating the intensity of the crises. This difference in FBD implementation (see "Methods" for other, more technical innovations) yields new results about the evolution of biodiversity in the OES grade. Notably, our new analyses contradict our previous conclusion (Didier and Laurin 2024) that the OES grade was not affected by mass extinction events. We thus confirm the existence of an extinction event around the Carboniferous/Permian boundary that we first detected among varanopids (Laurin and Didier 2025) and provide strong evidence that Olson's extinction (Lucas 2017; Brocklehurst 2018) had a strong impact on the OES grade in the Kungurian.

Compared with previous studies by others, our work introduces several types of improvements. First, the stratigraphic resolution of the database used is finer than stage level (Laurin and Didier 2025) while avoiding time binning, a strategy that can create artifacts, as explicitly acknowledged by Brocklehurst (2018), who used alternative strategies to minimize this problem. Second, we use phylogeny-informed analyses rather than taxon counts (e.g., Irmis and Whiteside 2012), because the latter is known to be suboptimal (Bertrand et al. 2006). Third, our analyses are performed at the lineage (species) level, rather than on families (e.g., Benton 1989) or genera (e.g., Day et al. 2015). Finally, our FBD-based method was especially designed to model biodiversity evolution using the fossil record in a phylogenetic context, whereas other implementations of the FBD (e.g., Heath et al. 2014) and other analytical methods do not fully use the stratigraphic and phylogenetic information that fossils can provide.

Methods

We updated the absolute age of the 175 fossil occurrences of the 50 terminal taxa considered by Didier and Laurin (2024) to reflect the geologic timescale (GTS from here on) published in September 2023 (Cohen et al. 2023), because Didier and Laurin (2024) had used an earlier timescale published by Gradstein and Ogg (2020). In most cases, the differences between these two GTSs are small for the relevant chronostratigraphic units, namely the interval between late Pennsylvanian and early Guadalupian. The sole exception is the Kungurian/Roadian boundary, which was placed at 274.4 Ma in the 2020 GTS, but was moved to 273.01 Ma in the 2023 GTS. These records were extracted both from the Paleobiology Database (Peters and McClennen 2016) and from the primary literature (see Didier and Laurin [2024] for the references).

We used the same tree population sample of 100 equiparsimonious trees as Didier and Laurin (2024). Analyses were carried out by using our current implementation of the skyline FBD model, a model for which other implementations are available (Gavryushkina et al. 2014; Zhang et al. 2016; do Rosario Petrucci et al. 2025). Under this model, lineages can undergo three types of events: speciation (cladogenesis), extinction, or fossilization with respective rates λ, μ, and ψ that are constant over a given number of time slices. Our current implementation, first used in our study of varanopid diversification (Laurin and Didier 2025), allows us to estimate both boundary times between the slices and the rates under user-defined constraints. For instance, one may constrain the fossilization rate to remain the same over all the slices, as we do here. We test models with up to three time slices and up to two mass extinction events. Didier and Laurin (2024) and older studies had tested only simpler models with no more than two time slices and a single extinction event, if any. Data required are the tree topology (without the divergence times) of the studied taxa, which may be extinct or not, and the fossil ages, generally provided as stratigraphic intervals. Our software handles missing data by dealing with the situation where the fate of certain lineages is unknown (or not considered for some reason) from a time specific to each of these lineages.

Some technical features of our software changed from the version used in Laurin and Didier (2025). In particular, the likelihood optimization now proceeds in two stages (rather than one), with a global search followed by a local refinement. This two-step approach is essential, because the maximum likelihood is not computed solely over the model parameters, but also over the fossil ages, which are themselves constrained by their stratigraphic intervals. We use the NLopt implementation of the evolutionary algorithm described in da Silva Santos et al. (2010) for the global stage, followed by the Subplex algorithm for the local optimization (Rowan 1990).

Results

Our new analyses support the existence of two mass extinction events, one of moderate intensity at the Carboniferous/Permian boundary and a more severe one in the mid-Kungurian. In this respect, the present results differ sharply from the model favored in our previous study on the OES grade, which featured no mass extinction event (Didier and Laurin 2024). In addition, our results also show stronger support for the best model, which receives an Akaike information criterion (AIC) weight of 0.95 (Table 1). In our previous studies that used the skyline FBD, the best model received AIC weights of 0.65 in Didier and Laurin (2024) for the OES grade and 0.64 (reduced dataset) to 0.74 (full dataset) for varanopids (Laurin and Didier 2025). Thus, the most-supported model here (M3EE; Fig. 2), which includes three time slices and two partial extinction events, is our central scenario. The other models need not be considered, given their low support (AIC weight $\leq$ 0.05). That well-supported model (M3EE; Table 1) infers boundaries between time slices at 298.9 Ma, precisely at the Carboniferous/Permian boundary (placed at 298.9 Ma in the 2023 GTS used here), and at 278.9 Ma, in the mid-Kungurian (Figs. 2, 3).

The Carboniferous/Permian extinction event recovered by the best-supported model (M3EE) is mild, with a survival probability of 0.527 (Table 1). Its presence is strongly supported, to the extent that the best-supported model without that event (M3NE) has a low AIC weight of 0.050. That moderately severe crisis also marks a distinct shift in diversification dynamics in the OES grade. Before that crisis, in the first modeled time slice, the difference (r) between cladogenesis (0.564) and extinction rates (0.278), yields a positive

https://doi.org/10.1017/pab.2026.10102 Published online by Cambridge University Press

https://doi.org/10.1017/pab.2026.10102 Published online by Cambridge University Press

Table 1. Fit of the various fossilized birth–death (FBD) models showing that the data strongly support three time slices, a mild extinction event at the end of the Gzhelian and a severe mass extinction event in the mid-Kungurian. The number in the model name indicates the number of time slices modeled; "N" indicates that no mass extinction is modeled between two time slices; "E" indicates that a mass extinction is modeled between two time slices; models with three time slices include two letters that indicate if an extinction is modeled or not between the first and second, and between the second and third time slices (respectively). The parameters for each time slice are listed in the following order: cladogenesis ("speciation"), extinction, fossilization (here assumed to be constant), and (when a mass extinction is modeled at the end of the time slice) survival rate. AIC, Akaike information criterion.

Model	M1	M2N	M2E	M3NN	M3NE	M3EN	M3EE
Log likelihood	−692.09	−668.452	−670.15	−659.639	−651.44	−657.92	−647.5
No. of parameters	3	6	7	9	10	10	11
AIC	1738.18	1696.89	1702.31	1685.26	1670.88	1683.85	1665.01
AIC weight	0.0000	0.0000	0.0000	0.0000	0.0504	0.0001	0.9495
Estimated parameters, 1st time slice	0.151, 0.150, 0.278	0.535, 0.308, 0.286	0.626, 0.370, 0.282, 0.962	0.640, 0.397, 0.286	0.599, 0.369, 0.294	0.538, 0.259, 0.282, 0.542	0.564, 0.278, 0.295, 0.527
Estimated time boundary		299.02	299.778	299.84	299.681	298.90	298.90
2nd time slice		0.058, 0.122, 0.286	0.056, 0.117, 0.282	0.057, 0.079, 0.286	0.063, 0.077, 0.294, 0.115	0.053, 0.063, 0.282	0.060, 0.060, 0.295, 0.113
Estimated time boundary				279.00	279.00	279.00	278.90
3rd time slice				0.000, 0.492, 0.286	0.000, 0.080, 0.294	0.000, 0.499, 0.282	0.000, 0.082, 0.295

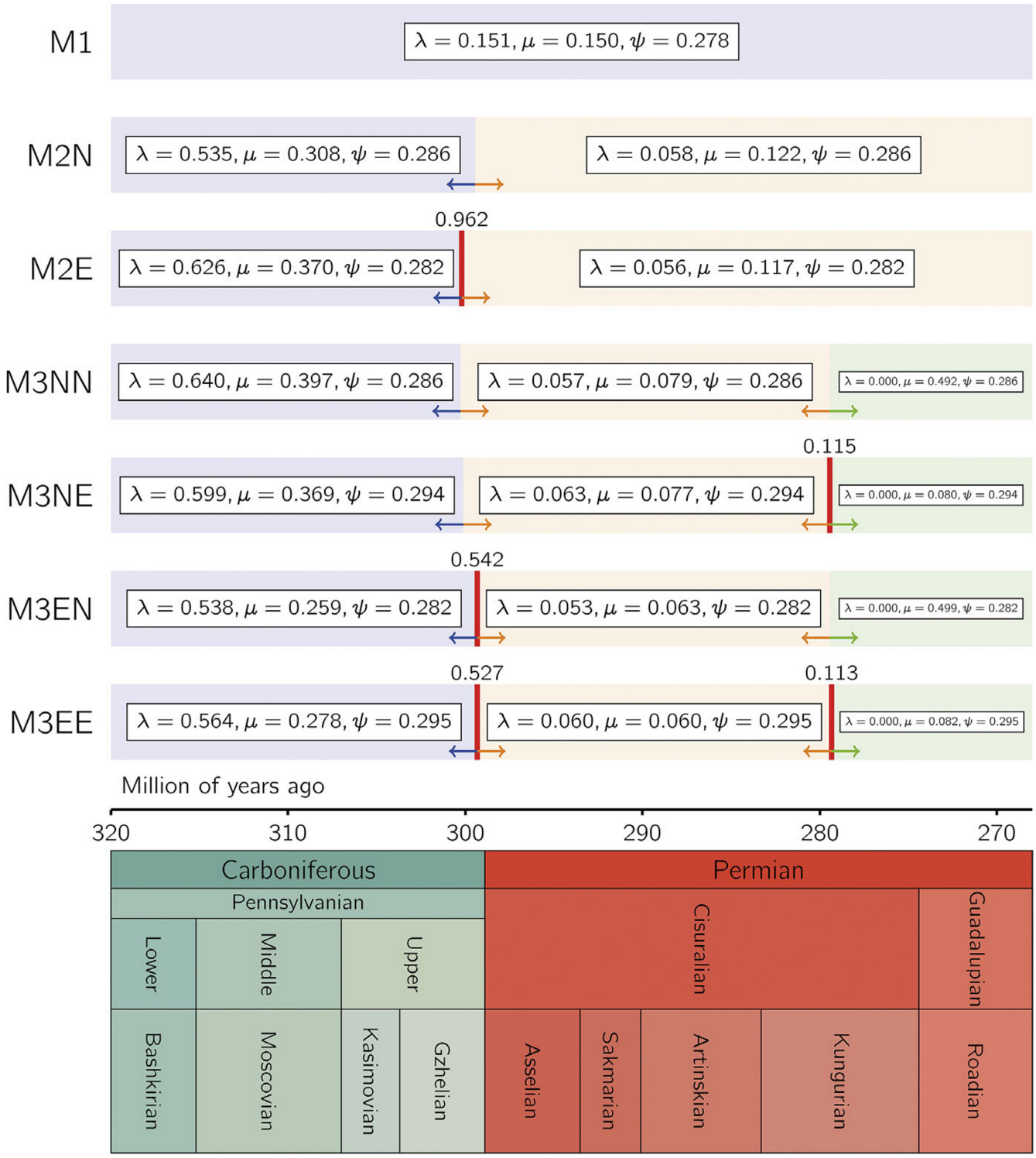


Figure 2. Models tested and parameter estimates. Following the "M" for "model," the number indicates how many time slices are considered. One or two letters follow for models that include two or three time slices, respectively. The letters "E" and "N" indicate the presence or not (respectively) of a mass extinction event at the time boundary between two slices. For models with two slices, there is a single such boundary. For models with three time slices, the first letter specifies whether a mass extinction is allowed (E) or not (N) between the two oldest slices, and the second letter specifies whether a mass extinction event is allowed (E) or not (N) between the two youngest slices. Mass extinction events are represented with thick vertical lines. The best-supported model, with an Akaike information criterion (AIC) weight of 0.95, is model M3EE (Table 1).

and fairly strong (0.286) net diversification rate. By contrast, after that crisis, in the second modeled time slice that represents most of the Cisuralian, the net diversification is nil (r = 0.000). This results from a drastic drop in the rate of cladogenesis to only 0.006, which is not fully compensated by a strong, but smaller drop in extinction rate to 0.006.

https://doi.org/10.1017/pab.2026.10102 Published online by Cambridge University Press

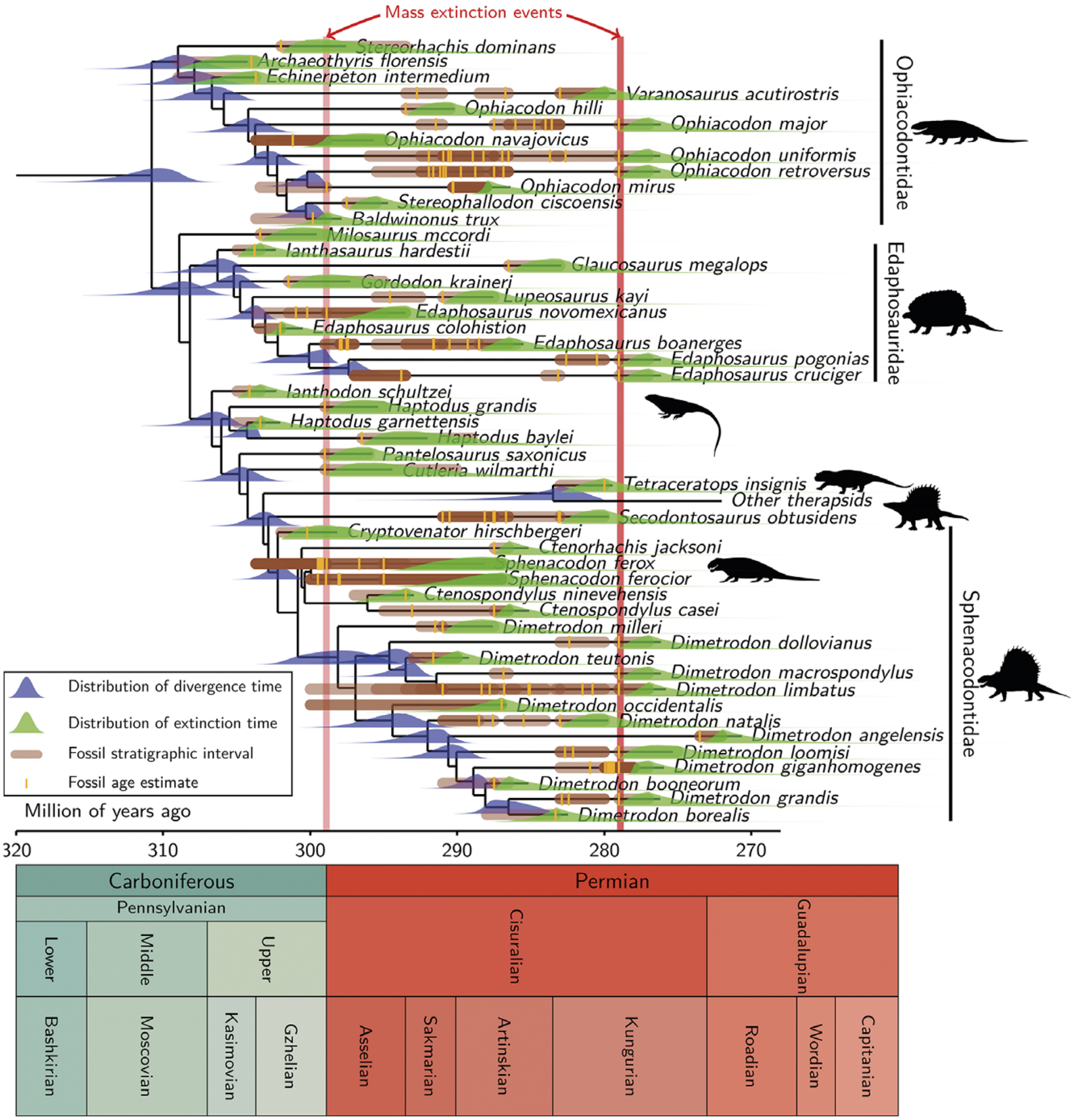


Figure 3. Timetree with modeled mass extinction events. This figure was generated using our computer program (https://github.com/gilles-didier/DateFBD). The probability densities of divergence times are shown in violet on one of the 100 most parsimonious trees used in our analyses; extinction time probability density for each lineage is shown in green. The fossil ages that maximize maximum likelihood under model M3EE are indicated by narrow orange vertical bars. Divergence and extinction time densities are computed from the single-slice model, without considering any mass extinction event (in which case the extinction distributions would be mixtures of a Dirac distribution at the time of the event and of another distribution similar to those plotted here—the first component of the mixture accounting for cases where the lineage is actually killed by the event, and the second for cases where it is not). The two vertical bars crossing the tree represent the mass extinction events supported by the most-supported model. Line transparency for extinction events is proportional to survival rate; hence, the most severe extinction corresponds to the darkest, most obvious line. The outlines of several taxa were downloaded from PhyloPic (https://www.phylopic.org/). These include, from top to bottom, *Ophiacodon uniformis* by Dmitry Bogdanov; *Edaphosaurus pogonias* by Matt Celeskey (Attribution 3.0 Unported); *Haptodus garnettensis* by Dmitry Bogdanov, vectorized by T. Michael Keesey; *Tetraceratops insignis* by Nobu Tamura, modified by T. Michael Keesey; *Secodontosaurus obtusidens* (CC0 1.0 Universal Public Domain Dedication); *Sphenacodon ferox* by Dmitry Bogdanov (Attribution-ShareAlike 3.0 Unported); and *Dimetrodon* by Alessio Ciaffi (Attribution 4.0 International). The *Ophiacodon*, *Haptodus*, *Tetraceratops*, and *Sphenacodon* illustrations were published under the Attribution-ShareAlike 3.0 Unported license.

The mid-Kungurian extinction event that affected the OES grade in model M3EE appears to be much more severe (Figs. 2, 3), with a survival rate of only 0.113. It is also better supported than the Carboniferous/Permian extinction event, given that the best-supported model without the Kungurian event (M3EN) barely reaches an AIC weight of 0.0001. After that crisis, in the third time

https://doi.org/10.1017/pab.2026.10102 Published online by Cambridge University Press

slice that represents the late Kungurian and at least the early Roadian, the background rate of biodiversity loss seems to have accelerated. This results from a sharp drop in the rate of cladogenesis (0.000) and a slight increase in the extinction rate, to 0.082 (Table 1), which yields a negative net diversification rate (r) of −0.082, as opposed to 0.000 in the previous time slice. However, given that very few lineages in the OES grade are represented in that third time slice, this estimate is poorly constrained. These taxa include minimally *Dimetrodon angelensis*, from the San Angelo Formation (Olson 1962), which probably dates from the early Roadian but could conceivably extend into the latest Kungurian (Laurin and Hook 2022). However, several other taxa from the OES grade may also extend into this time slice (Fig. 3). These additional taxa potentially include lineages whose latest known fossil occurrences fall entirely or partly (given the uncertainty over their exact age) in that time slice: six species of *Dimetrodon* (*D. grandis*, *D. giganhomogenes*, *D. loomisi*, *D. limbatus*, *D. macrospondylus*, and *D. dollovianus*), two species of *Edaphosaurus* (*E. cruciger* and *E. pogonias*), and three species of *Ophiacodon* (*O. retroversus*, *O. uniformis*, and *O. major*). Other OES grade taxa that may extend into this third time slice are those whose latest occurrence predates that time a bit, but whose extinction time probability densities (Fig. 3) do not allow us to rule out the possibility that they extended into that time slice. Among these we find the following taxa: *Varanosaurus acutirostris*, *Secodontosaurus obtusidens*, *Dimetrodon natalis*, and *Tetraceratops insignis*. The latest records of these taxa probably date from between 283 and 280 Ma, but they may well have become extinct after 278.9 Ma.

Discussion

Comparisons with Previous FBD-based Studies of Early Synapsid Diversification

Several differences with our previous study on biodiversity evolution in the OES grade can be explained by the fact that we (Didier and Laurin 2024) previously only compared support for models with one or two time slices and at most a single extinction event between the two time slices. Furthermore, the position of boundaries between time slices had to be determined a priori, and these boundaries were placed between successive geological stages. Thus, in Didier and Laurin (2024), the best-supported model (with an AIC weight of 0.65) had a limit between time slices at the Asselian/Sakmarian boundary, one geological stage later than found here. However, the second best-supported model in that study, with an AIC weight of 0.22 (about a third of the weight of the best-supported model) placed the limit between the two time slices at the Carboniferous/Permian boundary (298.9 Ma), as in our present estimate. This congruence is better than expected, given the age uncertainty that is associated with all fossil ages (the average range of possible ages of the 175 fossil occurrences is about 3.6 Myr). Similarly, the age and the exact stratigraphic position of the Carboniferous/Permian boundary in continental sediments has long been debated and remains uncertain, including in the basins from which the bulk of our OES data originates (Utting and Lucas 2010).

The boundary between the second and third time slices, in the mid-Kungurian (278.9 Ma), is marked by a fairly severe mass extinction event (survival probability of 0.113) in the OES grade (Figs. 2, 3). That extinction event could not be detected for methodological reasons in our previous study on varanopids (Laurin and Didier 2025) or on the OES grade (Didier and Laurin 2024). However, the existence of an extinction event around that time was first inferred long ago (Olson 1982). It was subsequently nicknamed "Olson's extinction" (Sahney and Benton 2008), and its existence is supported by a few more recent studies (Ruta and Benton 2008; Brocklehurst et al. 2013; Brocklehurst 2018, 2020). Our analytical method, which simultaneously maximizes likelihood of the model and of the age of each fossil within the specified age interval, as was already done in Didier and Laurin (2024), can push the ages of several fossils toward one of the specified age bounds. This happened here for several taxa (listed in the "Results") for which the latest occurrence could date from between 279 and 277 Ma. These occurrences are here estimated to have occurred between 278.86 and 279 Ma, an interval that ends at the inferred mid-Kungurian crisis (Fig. 3). Note that this result has some independent stratigraphic support, because as described in "The Pulse," the late Kungurian in both Texas and Oklahoma includes a large stratigraphic gap (of unknown exact duration) in the fossil record (Laurin and Hook 2022). That crisis may have been especially severe among synapsids, because it was partly responsible for the fairly quick, partial replacement of the presumably ectothermic Permo-Carboniferous synapsid clades by the apparently endothermic therapsids (de Ricqlès 1972; Faure-Brac and Cubo 2020; de Buffrénil et al. 2021).

The diversification dynamics inferred here for the OES grade shows a dramatic drop in the rate of cladogenesis and extinction between the first two time slices, as in Didier and Laurin (2024). However, we now infer two mass extinction events (see "Results") and a nil net diversification rate in the second time slice, rather than the slow decline inferred in our previous work. The discrepancy between these studies is due partly to the estimated boundaries (rather than fixed a priori) between time slices, which could explain the detection of a mid-Kungurian crisis. Didier and Laurin (2024) could not test that hypothesis, because extinction events were constrained to occur at stage boundaries. Another important methodological difference is the additional assumption made here that the fossilization rate is constant over the entire diversification period, as in Laurin and Didier (2025), whereas it was allowed to vary between time slices in Didier and Laurin (2024). This assumption is motivated by the difficulties encountered when maximizing the likelihood while allowing both the limit ages and the fossilization rates to vary. These technical difficulties generate instability in our estimates of limit ages, at least with datasets of moderate size such as ours (50 terminal taxa and 175 fossil occurrences). Constraining the fossilization rate to remain constant resolves this issue. Despite these numerical differences, both sets of estimates result in significantly positive diversification in the first time slice. Likewise, in the second time slice, both sets of estimates indicate a significant slowdown of diversification, although both studies differ in detail. Our new estimates of stagnating biodiversity over time (Fig. 2), with an r of about 0.000, contrasts with the biodiversity decline (r of about −0.078) inferred by Didier and Laurin (2024), who had estimated cladogenesis and extinction rates of 0.021 and 0.099, respectively. This difference in rate of biodiversity loss between both studies is readily explained by the fact that our new estimate incorporates a severe mass extinction in the Kungurian. In contrast, the impossibility of modeling such an event in our previous study resulted in a steeper rate of biodiversity loss as an alternative way to explain why the OES grade vanished from the fossil record around the Kungurian/Roadian boundary.

Comparisons with our recent results on varanopids are much easier, because Laurin and Didier (2025) used our current implementation of the FBD that estimated the boundary between time slices, and we tested for the presence of up to two mass extinction

https://doi.org/10.1017/pab.2026.10102 Published online by Cambridge University Press

events. Only two main caveats hamper these comparisons. The first is that because of the smaller size of the analyzed varanopid datasets (16 or 21 taxa with 31 or 36 fossil occurrences, as opposed to 50 taxa and 175 fossil occurrences here), no more than two time slices were modeled. A third time slice was allowed in some models, but its parameters were set arbitrarily, because there were no varanopid fossils in that time slice. The second caveat is that the fossil record of varanopids extends up to the Capitanian, whereas Ophiacodontidae and Edaphosauridae disappear from that record in the Kungurian, and Sphenacodontidae probably extends a bit longer into the early Roadian (Laurin and Hook 2022). Thus, there might be genuine differences in diversification dynamics between Varanopidae and the OES grade in the Pennsylvanian and Cisuralian, and comparisons are simply impossible in the Guadalupian, given that the OES grade left a negligible fossil record in that epoch.

With these caveats in mind, we note that for Varanopidae, Laurin and Didier (2025) estimated the boundary between the first two time slices close to the Carboniferous/Permian boundary, either synchronous with our current estimate (298.9 Ma) or about 2 Myr later (296.94 Ma). This was based on the two best-supported models in each varanopid datasets (full and reduced), which resulted in four estimated models. This confirms a significant change in diversification of all these eupelycosaurs around the Carboniferous/Permian boundary, if varanopids are indeed eupelycosaurs (see "Introduction").

Likewise, both studies find support for a moderate extinction event around the Carboniferous/Permian boundary, which as far as we know, was not previously reported (at least for vertebrates) in the literature. Our inferred survival rate of 0.527 for the OES grade translates into an extinction rate of 0.473, which is less severe than in the "big five" (or six) mass extinction events. The intensity of the latter is difficult to compare with our results, because the reported extinction rates are typically expressed for taxa of higher taxonomic levels (e.g., Labandeira 2005), but McGhee et al. (2013: table 3) reported that the six most severe extinction events had 39–83% extinction rates for genera. This would translate into specific extinction rates greater than 60%, according to the rarefaction curve proposed by Stanley (2016: fig. 5). In any case, this OES extinction rate is apparently about as high as in Varanopidae, for which Laurin and Didier (2025) estimated a survival rate of 0.747 on the exhaustive dataset (21 taxa), and only 0.358 for the reduced dataset (16 taxa). However, given the small sample size for Varanopidae, which is constrained by the small size of that clade, these numbers must be interpreted with caution. Our new analyses significantly strengthen the case for a moderate Carboniferous/Permian extinction event, given that the dataset of our OES grade dataset is about three times larger than the varanopid dataset.

Both sets of taxa seem to have stagnated or declined slowly in the Cisuralian (and, in the case of Varanopidae, until their final demise in the Capitanian). These rates of nil or negative diversification are very similar in both groups: $r = 0.000$ in the OES grade and $r = -0.013$ in Varanopidae. According to the models obtained here and by Laurin and Didier (2025), the fact that varanopids may not have been affected by the mid-Kungurian crisis could explain their much greater longevity.

The mid-Kungurian crisis apparently affected the OES grade much more than Varanopidae (Figs. 2, 3). The OES grade appears to have experienced a fairly severe crisis in the mid-Kungurian (a survival rate of only 0.113 translates into an extinction rate of 0.887) and to have become extinct shortly thereafter. Indeed, the last known lineage of that grade is *Dimetrodon angelensis* from the latest Kungurian to (more likely) early Roadian San Angelo Formation (Olson 1962; Laurin and Hook 2022). Of course, Therapsida had probably started their evolutionary radiation by then, and they are rooted in the OES grade in all recent phylogenies (e.g., Sidor 2001; Brocklehurst et al. 2022; Matamales-Andreu et al. 2024), but their physiology may have differed rather sharply from that of the OES grade (de Ricqlès 1972; Faure-Brac and Cubo 2020; de Buffrénil et al. 2021). On the contrary, we found no evidence of an extinction event in Varanopidae in the Kungurian, although the low sample size of fossil occurrences in that clade and the methodological caveats noted earlier make that conclusion tentative (Laurin and Didier 2025). The absence of a Kungurian extinction event among varanopids, if genuine, might be linked to their "somewhat more upland" environment, which they shared with Caseasauria, which also survived that event.

Note that the meaning of "upland" in vertebrate paleontology (at least for Permo-Carboniferous stegocephalians) has never been rigorously defined, as far as we know. For instance, the Bromacker locality of the Tambach Formation (Sakmarian or Artinskian) experienced periodic flooding, so streams and at least ephemeral bodies of standing water were present, but no large, perennial lake or river appears to have been present. Yet Bromacker is reputedly the best example of an "upland" locality in the Cisuralian (Eberth et al. 2000). Unsurprisingly, this concept has recently been criticized by paleobotanists (Bashforth et al. 2021). In this context, "upland" mostly means "farther from large, perennial water bodies" and does not necessarily imply high altitude, mountains, or even hills, even though the concept encompasses such habitats, at least potentially (Olson 1975). Nevertheless, this difference in habitat may explain the different fates of the OES grade compared with varanopids, especially if these differences in habitat resulted in different diets.

Comparisons with Previous Studies on Diversification in the Late Paleozoic

The change in diversification dynamics detected by the three recent FBD-based diversification studies of early synapsids (Didier and Laurin 2024; Laurin and Didier 2025; and the present one) around the Carboniferous/Permian boundary had not been discussed in the literature previously, but at least one recent study of marine metazoans found a similar pattern. Namely, Fan et al. (2020) described "a previously unrecognized great biodiversification event" that they called "the Carboniferous/Permian Biodiversification Event." As in our study, their species-level biodiversity curve (their fig. 1A) shows a diversification restricted to the Carboniferous (with a slight dip near the mid-Carboniferous that may be a modest extinction event) and a sudden drop in diversity in the earliest Permian. As in our new results, the Permian data of Fan et al. (2020) suggest no long-term biodiversity trend in most of the Cisuralian.

This similarity is surprising given the fact that the data used by Fan et al. (2020) come from marine organisms (without vertebrate data; the diversification events described in the "Results" are especially visible among brachiopods and foraminifera) and that they were largely derived from Chinese sections. By contrast, our dataset is restricted to a fairly small number of continental amniotes, chiefly from what is now western North America and Europe, which were then parts of equatorial Pangea, rather far from the blocks that now form China (Kent and Muttoni 2020). Thus, despite strong taxonomic, ecological, and geographic differences between these datasets, both studies (Fan et al. 2020 and the present one) point to a drop in diversity around the Carboniferous/Permian boundary. This point clearly deserves additional scrutiny.

https://doi.org/10.1017/pab.2026.10102 Published online by Cambridge University Press

Among the land plant communities, the Carboniferous/Permian boundary coincides with an increase in the relative abundance of xeromorphic, drought-tolerant floras alternating with hygromorphic, wetland taxa. This marks the appearance of so-called mixed floras (e.g., Falcon-Lang et al. 2015; DiMichele et al. 2014, 2019; Marchetti et al. 2022). That floral change may well have affected insects by potentially driving faunal turnover. This is indicated by the high values of insect origination and extinction rates estimated during the Upper Pennsylvanian, followed by an early Permian minimum and a subsequent renewed increase (Labandeira 2005; Nicholson et al. 2015). Given the dominance of phytophagy, fungivory, and detritivory in Paleozoic insect communities (Rainford and Mayhew 2015), shifts in floral composition from hygromorphic to xeromorphic taxa may have acted as primary driver of the observed insect dynamics, as observed during other large-scale biotic transitions (Jouault et al. 2022). Indeed, the detritivore-rich insect communities of the Middle Pennsylvanian were complemented in the Upper Pennsylvanian by the emergence of new herbivorous taxa. This is shown by the first occurrence of fossilized galls on petioles and tunnel-and-gallery networks on tree ferns (Labandeira and Phillips 1996, 2002), which indicates the establishment of more complex trophic interactions. Did these floral changes negatively affect the OES grade and varanopids?

A Press–Pulse Extinction Event or a Pulse–Press–Pulse Event?

The observed biodiversity pattern is reminiscent of (but not identical to) the general pattern of the press–pulse model proposed by Arens and West (2008). The press–pulse model predicts a prolonged decline (the press) followed by a brief crisis (the pulse). The pattern that we infer for the OES grade differs slightly from that, because instead of a press, we see a stagnating biodiversity lasting about 20 Myr (from about 299 to 279 Ma). While a 20 Myr stagnation in biodiversity might not seem like a strong signal, this contrasts rather sharply with the rapid diversification that took place in the Pennsylvanian, and this suggests that the environment (biotic or abiotic) was less favorable for the OES grade and varanopids. Furthermore, Didier and Laurin (2024) had inferred negative diversification, which matches the expected press. This is followed by a fairly severe extinction event (a survival probability of 11.3% translates into an extinction rate of 88.7%), which certainly qualifies as a pulse. However, we also observe a first pulse (with a survival probability of 52.7%), weaker than the second one, just before the press (Figs. 2, 3). Because of this, the pattern that we observe could better be called a "pulse–press–pulse."

In the original proposal of this model, Arens and West (2008) envisioned the press (a slow, long-lasting biodiversity decline) to generally be caused by a phase of intense volcanism and the pulse (a brief dramatic biodiversity loss) to be caused by the impact of a large asteroid. However, Arens and West (2008) indicated that other events might cause similar patterns; for instance, climate and sea-level changes could cause the press, whereas marine anoxic incursions could cause the pulse (in the seas).

Origin of the First Pulse

A plausible cause of this mild, Carboniferous/Permian extinction event might be a warming event as recorded in $\delta^{18}O_{apt}$ in conodonts from offshore sediments from South China (Chen et al. 2016). The 1‰ decrease in the oxygen isotope record corresponds to a maximum temperature rise of 4°C, although the increase may have been more moderate if accompanied by ice sheet melting (Chen et al. 2016). This is supported by the global sea-level curve during the Gzhelian (Haq and Schutter 2008), which shows a rise consistent with milder warming. This warming is also supported by vegetational changes (toward more arid-adapted land plants) that took place at the time (DiMichele et al. 2009). This warming could be due to the first phase of the Tarim and Skagerrak-centered large igneous provinces (LIPs), which have been dated at ~300 Ma (Xu et al. 2014) and 297.5 ± 3.8 Ma (Torsvik et al. 2008), respectively.

The Press

In the Cisuralian, the press could plausibly be attributed to a trend toward a warmer and more arid (at least seasonally) climate. This trend could be linked to the end of the LPIA with the waning of the glaciation covering the Southern Hemisphere and an increase in atmospheric pCO_2 levels from the early Cisuralian onward (e.g., Montañez and Poulsen 2013; Richey et al. 2020). The transition was not continuous but rather stepwise, and plausibly diachronous from west to east (e.g., Cleal and Thomas 2005; DiMichele et al. 2009, 2014; Richey et al. 2020). It probably lasted a long time; its earliest manifestation may be visible in the Kasimovian, a stage for which we have scant data on amniote diversity, probably because amniote diversification had begun only shortly before (Fig. 3). Sahney et al. (2010) argued that a rainforest collapse occurred at that time, resulting in dietary regime shifts among stegocephalians, and that this accelerated diversification, especially among amniotes. The initially high diversification of the OES grade that we detect here (as in Didier and Laurin 2024) is consistent with this interpretation. This climatic trend appears to have affected areas inhabited by the OES grade, because a flora adapted to a seasonally dry climate was reported in the Asselian of what is now New Mexico (Falcon-Lang et al. 2015). As the climate continued becoming warmer and drier (well into the mid- to late Cisuralian), diversification of eupelycosaurs slowed dramatically. This apparently occurred rather suddenly around the end of the Carboniferous.

The coeval rise in pCO_2 is possibly linked to volcanic events that took place mostly from the late Asselian to early Kungurian (Shellnutt et al. 2011; Xu et al. 2014; Wei et al. 2020). That activity was especially intense from the Sakmarian–Artinskian onward, with volcanic episodes such as the Tarim II, Tarim III, Panjal Traps, Qiangtang basalt, and Silicic Choiyoi igneous province (Ernst and Buchan 2001; Richey et al. 2020). Evidence from both western (e.g., Montañez et al. 2007; Poulsen et al. 2007; Montañez and Poulsen 2013; Richey et al. 2020) and central tropical Pangea low-latitude successions (e.g., Schneider et al. 2006, 2020; Marchetti et al. 2022) supports an intensification of the aridification trend and the following biotic turnover during the Artinskian warming episode (Forte et al. 2023).

This aridification process is documented by pedotypes in the Appalachian Basin, as surveyed by Hembree (2022) in the upper Pennsylvanian to lower Permian Conemaugh; Monongahela, and Dunkard groups in eastern North America; and ichnological and paleobotanical data from the Southern Alps, in northern Italy (Marchetti et al. 2022). This includes plant macro- and microfossil assemblages supporting dry, seasonal, and semiarid conditions and a decline in diversity and abundance among anamniotic stegocephalians from the Artinskian–Kungurian onward (e.g., Forte et al. 2018a,b; Marchetti et al. 2022; Vallé et al. 2023). This long-term aridification is further supported by a gradual temperature increase of a maximum of 2°C (Chen et al. 2013) and a global decrease in river input into the oceans as recorded by strontium ($^{87}Sr/^{86}Sr$)

https://doi.org/10.1017/pab.2026.10102 Published online by Cambridge University Press

(Korte et al. 2006; Wang et al. 2021) and lithium isotope (δ^7Li) ratios (Wang et al. 2024). A recently reported xerophytic Lopingian paleoflora from North America is also consistent with this inferred climatic trend (Hotton et al. 2025).

The fact that we did not detect an extinction event during the Artinskian warming episode may simply be a constraint linked to the fact that we tested models with up to three time slices and two extinction events only. This constraint is imposed by the amount of data that we have (on 50 taxa and 175 fossil occurrences) and, to a lesser extent, by their associated uncertainty (phylogenetic and geochronological). However, given that our model estimated the position of the diversification dynamics shifts, our results suggest that these changes were more substantial near the Carboniferous/Permian boundary and in the Kungurian than in the Artinskian. In future studies, when we have more data (i.e., on additional amniote clades), we will be able to test more complex models, at least if these clades seem to follow similar diversification patterns.

The climatic trend marked by increasing seasonality and aridity could also reflect a northward drift of the main continental fossiliferous basins of what had been equatorial Pangea in the Cisuralian into an arid zone located at slightly higher (tropical to subtropical) paleolatitudes of both hemispheres in the Guadalupian (Kent and Muttoni 2020). In that case, the inferred climatic change might be a local, rather than global, climatic trend. If so, as we recently suggested for varanopids (Laurin and Didier 2025), it is conceivable that representatives of the OES grade persisted in other regions that have been less intensively prospected for fossils. In fact, a possible example of such records has been documented in the Lopingian or Early Triassic Buena Vista Formation from Uruguay, which has yielded vertebrae that Piñeiro et al. (2003) argued belonged to a varanopid and, possibly, a sphenacodontid. At that time, the Buena Vista was located at a high, southern paleolatitude, outside the inferred arid latitudinal zones reconstructed by Kent and Muttoni (2020), so the climate should in any case have been humid enough to sustain early synapsid populations. Basal, ectothermic synapsids were not previously known in what is now South America, but such records were recently found (Angielczyk et al. 2026). This adds weight to the taxonomic interpretations of Piñeiro et al. (2003). However, the absence of the OES grade in the Guadalupian strata of two other high-latitude areas that have been intensively studied, namely the Russian Platform and the Karoo Basin, raises doubts about these putative late records of the OES grade. Caseids (Brocklehurst and Fröbisch 2017; Romano et al. 2018) and varanopids (Reisz and Berman 2001; Anderson and Reisz 2004) are known from the middle Permian of Russia, and the Karoo Basin has yielded varanopids (Modesto et al. 2011). All this suggests that the OES grade may well have been extinct by the late Wordian, or that the climate of these higher-latitude areas was unsuitable for the OES grade.

The Pulse

The cause of the pulse of extinctions in the mid-Kungurian (around 278 Ma) is probably a fast, global warming event that occurred at the end of the P2 glaciation, one of the glacial episodes of the LPIA. This mid-Kungurian interval is characterized by a global perturbation of the carbon cycle, evidenced by a prominent negative excursion (~3‰) in the carbon isotope record, hereafter referred to as the Kungurian carbon isotope excursion (KCIE; Liu et al. 2018; Huang et al. 2025). This isotopic anomaly is observed in both inorganic and organic carbon reservoirs and across marine and terrestrial environments. Its widespread occurrences, documented in South and North China (Liu et al. 2017; Lu et al. 2021; Fang et al. 2023), Venezuela and North America (Laya et al. 2013), South Africa (Van de Wetering et al. 2019), and eastern Australia (Birgenheier et al. 2010), supports its global extent.

The KCIE coincides with peaks in Hg/total organic carbon ratios, which suggests a link to enhanced volcanic activity (Lu et al. 2021). Notably, LIP activity in Tarim III and Qiangtang (Tibet) (Zhang and Zhang 2017), alongside contemporaneous arc volcanism in the Okhotsk-Taigonos and Choiyoi regions (Biakov 2012; Sato et al. 2015), has been dated to the time interval when our analyses place a mass extinction event (Fig. 4). However, carbon mass balance models indicate that volcanism alone cannot fully account for the magnitude of the KCIE (Liu et al. 2018). One plausible supplementary source is the release of isotopically light carbon from destabilized methane hydrates during the melting of the Gondwanan ice sheet (Liu et al. 2018; Huang et al. 2025).

Conodont δ^{18}O records show the onset of global warming in the early to mid-Kungurian (Chen et al. 2013). This warming, coupled with glacial melting, transgression, and the oxidation of released methane, likely contributed to widespread marine dysoxia and anoxia (Huang et al. 2025). Additionally, lithium isotope data—a proxy for silicate weathering intensity—reveal exceptionally high values during the Kungurian compared with the Asselian–Sakmarian and Capitanian–Changhsingian stages (Kalderon-Asael et al. 2021; Wang et al. 2024). The transition from a glacial to a more temperate climate likely intensified runoff and, together with elevated atmospheric CO_2, enhanced incongruent weathering that explains these high δ^7Li values.

In summary, the mid-Kungurian experienced a short-term but significant destabilization of the global carbon cycle, driven by volcanic emissions and possibly amplified by methane hydrate release. This provoked a rapid increase in pCO_2 and temperature which enhanced the hydrological cycle and increased river runoff. While this event has been documented mainly in the marine record until now, our study reveals a notable terrestrial response as well (Figs. 2–4).



Figure 4. One of the most recent *Dimetrodon* species (*D. grandis*, from the Kungurian Clear Fork Group; Reisz 1986) in front of a brightly colored sky, such as would have been produced by the intense volcanism that took place at the time. Even though much of the volcanism documented by the large igneous provinces (LIPs) was effusive, some explosive arc volcanism occurred in the Okhotsk-Taigonos and Choiyoi regions (Biakov 2012; Sato et al. 2015), and caldera eruptions occurred in the Southern Alps, in what is now northern Italy (Morelli et al. 2007, 2012; Marocchi et al. 2008; Willcock et al. 2013, 2015). Reconstruction by Dmitry Bogdanov, sky and digital manipulation by Roman Yevseyev (a photo editor and paleo-artist from Moscow, Russia), sent to us by Amin Khaleghparast, who suggested the colorful sky; all these individuals gave us permission to publish it.

https://doi.org/10.1017/pab.2026.10102 Published online by Cambridge University Press

This short-lived carbon cycle disruption corresponds to the start of a longer-term climatic shift away from glacial conditions, with subsequent glacial intervals (P3: late Kungurian to latest Roadian; P4: late Wordian to late Capitanian) reflecting more localized glaciation and reduced ice volume (Chen et al. 2013).

However, the apparent Kungurian mass extinction event might not be directly linked to the abovementioned climatic disturbances. Instead, it may be local and may result from a northward drift of the areas that yielded fossils of the OES grade (see "The Press"). Indeed, the fact that the bulk of the data on the OES grade comes from southwestern United States raises the possibility that the apparent extinction event is a taphonomic artifact. The upper part of the Clear Fork Formation (considered a group in the older literature) and the basal part of the San Angelo Formation, both in Texas, are rich in evaporites and were not conducive to fossilization (Presley and McGillis 1982); they have yielded no vertebrate fossils. A coeval gap occurs in Oklahoma, as Olson (1967) noticed long ago. Altogether, these barren strata in the late Kungurian and possibly earliest Roadian in Texas amount to a thickness of about 130 m (Laurin and Hook 2022). Olson (1967: 91) reported that the coeval fossil gap in Oklahoma is represented by "several hundred to nearly 1,000 feet of section between the Hennessey beds and the fossiliferous Chickasha beds." More fieldwork in late Kungurian continental basins would be useful to untangle possible taphonomic effects from a genuine mass extinction event at that time. Alternatively, similar analyses of biodiversity evolution on other, geographically more widespread clades of amniotes and other continental taxa in the late Kungurian could shed additional light on this matter.

At least two other studies on biodiversity evolution of early amniotes may be relevant to begin to address this issue. The first study assessed rates of morphological evolution in captorhinids (Brocklehurst 2017). While not focused on biological crises, that study showed a clear, spectacular drop in morphological disparity of Captorhinidae in the late Kungurian to early Roadian. The second, more relevant study used tip dating to try to discriminate between two hypotheses (Olson's gap or Olson's extinction) to explain the stratigraphic distribution of Permo-Carboniferous amniotes, using three datasets (one on amniotes, one concentrating on captorhinids, and a last one on caseids). That study concluded that the analyses "overwhelmingly" supported the hypothesis of an extinction (Brocklehurst 2017). Some of the data in these two studies could be affected by the same taphonomic factors as our data. However, both captorhinids and caseids extend beyond the early Roadian, and their Guadalupian distribution is documented in other areas, such as Russia (Maddin et al. 2008; Brocklehurst and Fröbisch 2017), China (Reisz et al. 2011), Niger (de Ricqlès and Taquet 1982), and Morocco (Jalil and Dutuit 1996). We also note that Olson's gap and Olson's extinction, which are often presented as mutually exclusive explanations of the observed stratigraphic range of amniotes in the Kungurian and Roadian, could coexist, because a genuine extinction event could occur just before a gap in the fossil record. Such a coincidence would challenge paleontologists, but geochronological (especially biostratigraphic) studies appear to rule out the existence of Olson's gap (Reisz and Laurin 2001, 2002; Lozovsky 2005; Benton 2012; Brocklehurst et al. 2017; Brocklehurst 2020; Laurin and Hook 2022). Thus, while these studies do not fully address the taphonomic problem that may affect our OES dataset, they do support our tentative conclusion that an extinction event took place in the Kungurian.

The fossil record in the marine realm, which is much more geographically widespread and stratigraphically continuous than that of continental vertebrates, is also relevant here. Biakov (2012) recognized a late Kungurian mass extinction event in northeast Asia; he documented species-level extinction rates of 78% for bivalves, 86% for brachiopods, and 60% for foraminifera. These data tip the balance in favor of a Kungurian mass extinction event in the OES grade, even though more research is needed to settle this question more conclusively.

Conclusion

Our new analyses confirm the presence of a mild extinction event near the Carboniferous/Permian boundary in synapsids, which we initially detected in varanopids (Laurin and Didier 2025), but which apparently also affected the OES grade. Climatic and floristic changes around that time may explain this mild crisis. Diversification of the OES grade stopped at that time, perhaps because of global warming and aridification throughout the Cisuralian, as the LPIA waned. We detect a strong mid-Kungurian crisis in the OES grade, which we did not detect (perhaps because of technical limitations and the low sample size) among varanopids. That crisis may result from rapid global warming linked partly to intensive volcanism (Fig. 4). The observed biodiversity pattern may represent a pulse–press–pulse pattern, reminiscent of the simpler press–pulse pattern that may characterize many mass extinction events, according to Arens and West (2008). Ancient mass extinction events, which provide a deep-time perspective on biodiversity loss, deserve careful study based on sophisticated analytical methods and datasets incorporating detailed stratigraphic and phylogenetic data. Such studies may improve our understanding of the current, anthropogenic biodiversity crisis, which constitutes a major societal challenge (Wake and Vredenburg 2008; Barnosky et al. 2011; Ceballos et al. 2015, 2017).

Acknowledgments. The authors thank D. Bogdanov (Chelyabinsk, Russia), who drew Figures 1 and 3; R. Yevseyev (Moscow, Russia), who reworked part of Figure 4; and A. Khaleghparast (Tehran, Iran) for establishing the contact between one of us (M.L.) and D. Bogdanov All these individuals gave us permission to publish these images. We thank two anonymous reviewers for their suggestions to improve the article. This work was supported by the recurring grants to the CR2P from the French ministry of research, the CNRS and Sorbonne Université (M.L.). This is the Paleobiology Database (PBDB) contribution number 550.

Competing Interests. The authors declare no conflicts of interest.

Data Availability Statement. The data used in this paper are available at https://doi.org/10.5061/dryad.qfttdz0x8. The code (along with the data) is available at https://github.com/gilles-didier/TimePiecewiseFBD2.

Literature Cited

Anderson, J. S., and R. R. Reisz. 2004. *Pyozia mesenensis*, a new, small varanopid (Synapsida, Eupelycosauria) from Russia: "pelycosaur" diversity in the Middle Permian. *Journal of Vertebrate Paleontology* **24**:173–179.

Angielczyk, K. D., and C. F. Kammerer. 2018. Non-mammalian synapsids: the deep roots of the mammalian family tree. Pp. 117–198 *in* F. Zachos and R. Asher, eds. *Mammalian evolution, diversity and systematics*. De Gruyter, Berlin.

Angielczyk, K. D., J. Fröbisch, C. F. Kammerer, R. M. Smith, C. A. Marsicano, J. D. Pardo, M. Richter, and J. C. Cisneros. 2026. Early synapsids from the Cisuralian (lower Permian) Pedra de Fogo Formation, Parnaíba Basin, Brazil: the first definitive South American "pelycosaurs." *Journal of Vertebrate Paleontology* **45**:e2621685.

Arefifard, S., and J. L. Payne. 2020. End-Guadalupian extinction of larger fusulinids in central Iran and implications for the global biotic crisis. *Palaeogeography, Palaeoclimatology, Palaeoecology* **550**:109743.

https://doi.org/10.1017/pab.2026.10102 Published online by Cambridge University Press

Arens, N. C., and I. D. West. 2008. Press-pulse: a general theory of mass extinction? *Paleobiology* **34**:456–471.

Barnosky, A. D., N. Matzke, S. Tomiya, G. O. Wogan, B. Swartz, T. B. Quental, C. Marshall, J. L. McGuire, E. L. Lindsey, and K. C. Maguire. 2011. Has the Earth's sixth mass extinction already arrived? *Nature* **471**:51–57.

Bashforth, A. R., W. A. DiMichele, C. F. Eble, H. J. Falcon-Lang, C. V. Looy, and S. G. Lucas. 2021. The environmental implications of upper Paleozoic plant-fossil assemblages with mixtures of wetland and drought-tolerant taxa in tropical Pangea. *Geobios* **68**:1–45.

Benoit, J., D. P. Ford, J. A. Miyamae, and I. Ruf. 2021. Can maxillary canal morphology inform varanopid phylogenetic affinities? *Acta Palaeontologica Polonica* **66**:389–393.

Benton, M. J. 1985. Mass extinction among non-marine tetrapods. *Nature* **316**: 811–814.

Benton, M. J. 1989. Mass extinctions among tetrapods and the quality of the fossil record. *Philosophical Transactions of the Royal Society B* **325**:369–386.

Benton, M. J. 2012. No gap in the Middle Permian record of terrestrial vertebrates. *Geology* **40**:339–342.

Bertrand, Y., F. Pleijel, and G. W. Rouse. 2006. Taxonomic surrogacy in biodiversity assessments, and the meaning of Linnaean ranks. *Systematics and Biodiversity* **4**:149–159.

Biakov, A. 2012. Permian biospheric events in Northeast Asia. *Stratigraphy and Geological Correlation* **20**:199–210.

Birgenheier, L. P., T. D. Frank, C. R. Fielding, and M. C. Rygel. 2010. Coupled carbon isotopic and sedimentological records from the Permian system of eastern Australia reveal the response of atmospheric carbon dioxide to glacial growth and decay during the late Palaeozoic Ice Age. *Palaeogeography, Palaeoclimatology, Palaeoecology* **286**:178–193.

Blob, R. W. 2001. Evolution of hindlimb posture in nonmammalian therapsids: biomechanical tests of plaeontological hypotheses. *Paleobiology* **27**:14–38.

Brink, K. S., M. J. MacDougall, and R. R. Reisz. 2019. *Dimetrodon* (Synapsida: Sphenacodontidae) from the cave system at Richards Spur, OK, USA, and a comparison of Early Permian–aged vertebrate paleoassemblages. *Science of Nature* **106**(1–2):2.

Brocklehurst, N. 2017. Rates of morphological evolution in Captorhinidae: an adaptive radiation of Permian herbivores. *PeerJ* **5**:e3200.

Brocklehurst, N. 2018. An examination of the impact of Olson's extinction on tetrapods from Texas. *PeerJ* **6**:e4767.

Brocklehurst, N. 2020. Olson's Gap or Olson's Extinction? A Bayesian tip-dating approach to resolving stratigraphic uncertainty. *Proceedings of the Royal Society B* **287**:20200154.

Brocklehurst, N., and J. Fröbisch. 2017. A re-examination of the enigmatic Russian tetrapod *Phreatophasma aenigmaticum* and its evolutionary implications. *Fossil Record* **20**:87–93.

Brocklehurst, N., C. F. Kammerer, and J. Fröbisch. 2013. The early evolution of synapsids, and the influence of sampling on their fossil record. *Paleobiology* **39**:470–490.

Brocklehurst, N., M. O. Day, B. S. Rubidge, and J. Fröbisch. 2017. Olson's Extinction and the latitudinal biodiversity gradient of tetrapods in the Permian. *Proceedings of the Royal Society B* **284**:20170231. http://doi.org/10.1098/rspb.2017.0231

Brocklehurst, N., D. Ford, and R. B. Benson. 2022. Early origins of divergent patterns of morphological evolution on the mammal and reptile stem-lineages. *Systematic Biology* **71**:1195–1209.

Carroll, R. L. 1988. *Vertebrate paleontology and evolution*. Freeman, New York.

Ceballos, G., P. R. Ehrlich, A. D. Barnosky, A. García, R. M. Pringle, and T. M. Palmer. 2015. Accelerated modern human–induced species losses: entering the sixth mass extinction. *Science Advances* **1**:e1400253.

Ceballos, G., P. R. Ehrlich, and R. Dirzo. 2017. Biological annihilation via the ongoing sixth mass extinction signaled by vertebrate population losses and declines. *Proceedings of the National Academy of Sciences USA* **114**:E6089–E6096.

Chen, B., M. M. Joachimski, S.-z. Shen, L. L. Lambert, X.-l. Lai, X.-d. Wang, J. Chen, and D.-x. Yuan. 2013. Permian ice volume and palaeoclimate history: oxygen isotope proxies revisited. *Gondwana Research* **24**:77–89.

Chen, B., M. M. Joachimski, X.-d. Wang, S.-z. Shen, Y.-p. Qi, and W.-k. Qie. 2016. Ice volume and paleoclimate history of the Late Paleozoic Ice Age from conodont apatite oxygen isotopes from Naqing (Guizhou, China). *Palaeogeography, Palaeoclimatology, Palaeoecology* **448**:151–161.

Cleal, C. J., and B. A. Thomas. 2005. Palaeozoic tropical rainforests and their effect on global climates: is the past the key to the present? *Geobiology* **3**:13–31.

Cohen, K. M., D. Harper, P. Gibbard, and N. Car. 2023. *International Chronostratigraphic Chart*. International Commission on Stratigraphy. www.stratigraphy.org.

da Silva Santos, C. H., M. S. Goncalves, and H. E. Hernandez-Figueroa. 2010. Designing novel photonic devices by bio-inspired computing. *IEEE Photonics Technology Letters* **22**:1177–1179.

Day, M. O., J. Ramezani, S. A. Bowring, P. M. Sadler, D. H. Erwin, F. Abdala, and B. S. Rubidge. 2015. When and how did the terrestrial mid-Permian mass extinction occur? Evidence from the tetrapod record of the Karoo Basin, South Africa. *Proceedings of the Royal Society B* **282**:20150834.

de Buffrénil, V., A. J. de Ricqlès, L. Zylberberg, K. Padian, M. Laurin, and A. Quilhac, eds. 2021. *Vertebrate skeletal histology and paleohistology*. CRC Press, Boca Raton, Fla.

de Ricqlès, A. 1972. Recherches paléohistologiques sur les os longs des tétrapodes III. — Titanosuchiens, dinocéphales et dicynodontes. *Annales de Paléontologie* **58**:17–60.

de Ricqlès, A., and P. Taquet. 1982. La faune de vertébrés du Permien Supérieur du Niger I. Le captorhinomorphe *Moradisaurus grandis* (Reptilia, Cotylosauria)—le crâne. *Annales de paléontologie* **68**:33–106.

Didier, G., and M. Laurin. 2021. Distributions of extinction times from fossil ages and tree topologies: the example of some mid-Permian synapsid extinctions. *PeerJ* **9**:e12577.

Didier, G., and M. Laurin. 2024. Testing extinction events and temporal shifts in diversification and fossilization rates through the skyline Fossilized Birth-Death (FBD) model: the example of some mid-Permian synapsid extinctions. *Cladistics* **40**:282–306.

DiMichele, W. A. 2014. Wetland-dryland vegetational dynamics in the Pennsylvanian ice age tropics. *International Journal of Plant Sciences* **175**:123–164.

DiMichele, W. A., I. Montañez, C. J. Poulsen, and N. J. Tabor. 2009. Climate and vegetational regime shifts in the late Paleozoic ice age earth. *Geobiology* **7**: 200–226.

DiMichele, W. A., C. L. Hotton, C. V. Looy, and R. W. Hook. 2019. Paleoecological and paleoenvironmental interpretation of three successive macrofloras and palynofloras from the Kola Switch locality, lower Permian (Archer City Formation, Bowie Group) of Clay County, Texas, USA. *PalZ* **93**: 423–451.

do Rosario Petrucci, B., M. R. May, and T. A. Heath. 2025. Fossils improve extinction-rate estimates under state-dependent diversification models. *Philosophical Transactions of the Royal Society B* **380**:20230313.

Eberth, D. A., D. S. Berman, M. Sumida, and H. Hopf. 2000. Lower Permian terrestrial paleoenvironments and vertebrate paleoecology of the Tambach basin (Thuringia, Central Germany): the Upland Holy Grail. *Palaios* **15**: 293–313.

Ernst, R. E., and K. L. Buchan. 2001. Large mafic magmatic events through time and links to mantle-plume heads. *Geological Society of America Special Papers* **352**:483–575.

Falcon-Lang, H. J., S. G. Lucas, H. Kerp, K. Krainer, I. P. Montañez, D. Vachard, D. S. Chaney, S. D. Elrick, D. L. Contreras, and F. Kurzawe. 2015. Early Permian (Asselian) vegetation from a seasonally dry coast in western equatorial Pangea: paleoecology and evolutionary significance. *Palaeogeography, Palaeoclimatology, Palaeoecology* **433**:158–173.

Fan, J.-x., S.-z. Shen, D. H. Erwin, P. M. Sadler, N. MacLeod, Q.-m. Cheng, X.-d. Hou, J. Yang, X.-d. Wang, and Y. Wang. 2020. A high-resolution summary of Cambrian to Early Triassic marine invertebrate biodiversity. *Science* **367**:272–277.

Fang, C., C. Zhang, X. Bai, H. Tang, J. Chao, and H. Wei. 2023. Facies and carbon isotope variations during the Kungurian (Early Permian) in the Chihsia Formation in the Lower Yangtze Region of South China. *Minerals* **13**:551.

Faure-Brac, M. G., and J. Cubo. 2020. Were the synapsids primitively endotherms? A palaeohistological approach using phylogenetic eigenvector maps. *Philosophical Transactions of the Royal Society B* **375**:20190138.

Felice, R. N., and K. D. Angielczyk. 2014. Was *Ophiacodon* (Synapsida, Eupelycosauria) a swimmer? A test using vertebral dimensions. Pp. 25–51 *in* C. F. Kammerer, K. D. Angielczyk, and J. Fröbisch, eds. *Early evolutionary history of the Synapsida*. Springer, Dordrecht, Netherlands.

https://doi.org/10.1017/pab.2026.10102 Published online by Cambridge University Press

Fielding, C. R., S. E. Bryan, J. L. Crowley, T. D. Frank, M. T. Hren, C. Mays, S. McLoughlin, J. Shen, P. J. Wagner, and A. Winguth. 2023. A multidisciplinary approach to resolving the end-Guadalupian extinction. *Evolving Earth* **1**:100014.

Ford, D. P., and R. B. Benson. 2020. The phylogeny of early amniotes and the affinities of Parareptilia and Varanopidae. *Nature Ecology and Evolution* **4**: 57–65.

Forte, G., E. Kustatscher, J. H. van Konijnenburg-van Cittert, C. V. Looy, and H. Kerp. 2017. Conifer diversity in the Kungurian of Europe—evidence from dwarf-shoot morphology. *Review of Palaeobotany and Palynology* **244**:308–315.

Forte, G., E. Kustatscher, J. H. van Konijnenburg-van Cittert, and H. Kerp. 2018a. Sphenopterid diversity in the Kungurian of Tregiovo (Trento, NE-Italy). *Review of Palaeobotany and Palynology* **252**:64–76.

Forte, G., E. Kustatscher, G. Roghi, and N. Preto. 2018b. The Permian (Kungurian, Cisuralian) palaeoenvironment and palaeoclimate of the Tregiovo Basin, Italy: palaeobotanical, palynological and geochemical investigations. *Palaeogeography, Palaeoclimatology, Palaeoecology* **495**:186–204.

Forte, G., F. Vallé, and E. Kustatscher. 2023. Unveiling the evolution of the Kungurian (Cisuralian) flora in the paleotropics (Southern Alps, Northern Italy). *Review of Palaeobotany and Palynology* **318**:104984.

Gavryushkina, A., D. Welch, T. Stadler, and A. J. Drummond. 2014. Bayesian inference of sampled ancestor trees for epidemiology and fossil calibration. *PLoS Computational Biology* **10**:e1003919.

Golubev, V. 2015. Dinocephalian stage in the history of the Permian tetrapod fauna of Eastern Europe. *Paleontological Journal* **49**:1346–1352.

Gônet, J., J. Bardin, M. Girondot, J. R. Hutchinson, and M. Laurin. 2023. Unravelling the postural diversity of mammals: contribution of humeral cross-sections to palaeobiological inferences. *Journal of Mammalian Evolution* **30**:321–337.

Gradstein, F., and J. Ogg. 2020. The chronostratigraphic scale. Pp. 21–32 *in* F. M. Gradstein, J. G. Ogg, M. D. Schmitz, and G. M. Ogg, eds. *Geologic Time Scale 2020*. Elsevier, Amsterdam.

Haq, B. U., and S. R. Schutter. 2008. A chronology of Paleozoic sea-level changes. *Science* **322**:64–68.

Heath, T. A., J. P. Huelsenbeck, and T. Stadler. 2014. The fossilized birth-death process for coherent calibration of divergence-time estimates. *Proceedings of the National Academy of Sciences USA* **111**:E2957–E2966.

Hembree, D. I. 2022. Early effects of the Late Paleozoic climate transition on soil ecosystems of the Appalachian Basin (Conemaugh, Monongahela, and Dunkard Groups): evidence from ichnofossils. *Palaios* **37**:671–690.

Hochuli, P. A., A. Sanson-Barrera, E. Schneebeli-Hermann, and H. Bucher. 2016. Severest crisis overlooked—Worst disruption of terrestrial environments postdates the Permian–Triassic mass extinction. *Scientific Reports* **6**: 28372.

Hotton, C. L., A. Bercovici, C. V. Looy, I. A. Duijnstee, D. S. Chaney, C. F. Eble, I. P. Montañez, S. Bourquin, B. Cecil, and J. Nelson. 2025. A late Permian palynological assemblage from the Spearfish Formation of South Dakota, United States: implications for biostratigraphy, paleofloristics, and phytogeography. *Palaeogeography, Palaeoclimatology, Palaeoecology* **679**: 113218.

Huang, G., S. Sun, A. Chen, J. G. Ogg, M. Hou, Q. Li, W. Li, and R. Yong. 2025. Shallow marine redox fluctuations of Yangtze Platform during the Cisuralian-Guadalupian transition: implications for Kungurian Carbon Isotope Excursion event. *Palaeogeography, Palaeoclimatology, Palaeoecology* **661**:112734.

Huttenlocker, A. K., S. A. Singh, A. C. Henrici, and S. S. Sumida. 2021. A Carboniferous synapsid with caniniform teeth and a reappraisal of mandibular size-shape heterodonty in the origin of mammals. *Royal Society Open Science* **8**:211237.

Irmis, R. B., and J. H. Whiteside. 2012. Delayed recovery of non-marine tetrapods after the end-Permian mass extinction tracks global carbon cycle. *Proceedings of the Royal Society B* **279**:1310–1318.

Jalil, N.-E., and J.-M. Dutuit. 1996. Permian captorhinid reptiles from the Argana Formation, Morocco. *Palaeontology* **39**:907–918.

Jenkins, X., R. B. Benson, D. P. Ford, C. Browning, V. Fernandez, K. Dollman, T. Gomes, E. Griffiths, J. N. Choiniere, and B. R. Peecook. 2024. Stepwise assembly of crown reptile anatomy clarified by late Paleozoic outgroups of Neodiapsida. bioRxiv:2024.11. 25.625221.

Jouault, C., A. Nel, V. Perrichot, F. Legendre, and F. L. Condamine. 2022. Multiple drivers and lineage-specific insect extinctions during the Permo–Triassic. *Nature Communications* **13**:7512.

Kalderon-Asael, B., J. A. Katchinoff, N. J. Planavsky, A. v.S. Hood, M. Dellinger, E. J. Bellefroid, D. S. Jones, A. Hofmann, F. O. Ossa, and F. A. Macdonald. 2021. A lithium-isotope perspective on the evolution of carbon and silicon cycles. *Nature* **595**:394–398.

Kent, D. V., and G. Muttoni. 2020. Pangea B and the Late Paleozoic ice age. *Palaeogeography, Palaeoclimatology, Palaeoecology* **553**:109753.

Korte, C., T. Jasper, H. W. Kozur, and J. Veizer. 2006. $^{87}Sr/^{86}Sr$ record of Permian seawater. *Palaeogeography, Palaeoclimatology, Palaeoecology* **240**:89–107.

Labandeira, C. C. 2005. The fossil record of insect extinction: new approaches and future directions. *American Entomologist* **51**:14–29.

Labandeira, C. C., and T. Phillips. 1996. A Carboniferous insect gall: insight into early ecologic history of the Holometabola. *Proceedings of the National Academy of Sciences USA* **93**:8470–8474.

Labandeira, C. C., and T. L. Phillips. 2002. Stem borings and petiole galls from Pennsylvanian tree ferns of Illinois, USA: implications for the origin of the borer and galler functional-feeding-groups and holometabolous insects. *Palaeontographica Abteilung A* **264**(1–4):1–84.

Laurin, M. 2010. *How vertebrates left the water*. University of California Press, Berkeley.

Laurin, M., and V. de Buffrénil. 2016. Microstructural features of the femur in early ophiacodontids: a reappraisal of ancestral habitat use and lifestyle of amniotes. *Comptes Rendus Palevol* **15**:115–127.

Laurin, M., and G. Didier. 2025. The rise and fall of Varanopidae† (Amniota, Synapsida). *Frontiers in Earth Science* **13**:1544451.

Laurin, M., and R. Hook. 2022. The age of North America's youngest Paleozoic continental vertebrates: a review of data from the Middle Permian Pease River (Texas) and El Reno (Oklahoma) Groups. *Bulletin de la Société Géologique de France* **193**(10):1–30.

Laurin, M., and G. Piñeiro. 2018. Response: commentary: a reassessment of the taxonomic position of mesosaurs, and a surprising phylogeny of early amniotes. *Frontiers in Earth Science* **6**(220):1–9.

Laya, J. C., M. E. Tucker, D. R. Gröcke, and A. Perez-Huerta. 2013. Carbon, oxygen and strontium isotopic composition of low-latitude Permian carbonates (Venezuelan Andes): climate proxies of tropical Pangea. *Geological Society of London Special Publication* **376**:367–385.

Liu, C., E. Jarochowska, Y. Du, D. Vachard, and A. Munnecke. 2017. Stratigraphical and $\delta^{13}C$ records of Permo-Carboniferous platform carbonates, South China: responses to late Paleozoic icehouse climate and icehouse–greenhouse transition. *Palaeogeography, Palaeoclimatology, Palaeoecology* **474**:113–129.

Liu, C., Y. Du, E. Jarochowska, J. Yan, A. Munnecke, and G. Lu. 2018. A major anomaly in the carbon cycle during the late Cisuralian (Permian): timing, underlying triggers and implications. *Palaeogeography, Palaeoclimatology, Palaeoecology* **491**:112–122.

Lozovsky, V. R. 2005. Olson's gap or Olson's bridge, that is the question. *In The Nonmarine Permian*. *New Mexico Museum of Natural History and Science Bulletin* **30**:179–184.

Lu, J., K. Zhou, M. Yang, P. Zhang, L. Shao, and J. Hilton. 2021. Records of organic carbon isotopic composition ($\delta^{13}C_{org}$) and volcanism linked to changes in atmospheric pCO_2 and climate during the Late Paleozoic Icehouse. *Global and Planetary Change* **207**:103654.

Lucas, S. G. 2009. Timing and magnitude of tetrapod extinctions across the Permo-Triassic boundary. *Journal of Asian Earth Sciences* **36**:491–502.

Lucas, S. G. 2017. Permian tetrapod extinction events. *Earth-Science Reviews* **170**:31–60.

MacDougall, M. J., S. P. Modesto, N. Brocklehurst, A. Verrière, R. R. Reisz, and J. Fröbisch. 2018. Commentary: a reassessment of the taxonomic position of mesosaurs, and a surprising phylogeny of early amniotes. *Frontiers in Earth Science* **6**:99.

Maddin, H. C., C. A. Sidor, and R. R. Reisz. 2008. Cranial anatomy of *Ennatosaurus tecton* (Synapsida: Caseidae) from the Middle Permian of Russia and the evolutionary relationships of Caseidae. *Journal of Vertebrate Paleontology* **28**:160–180.

Marchetti, L., G. Forte, E. Kustatscher, W. A. DiMichele, S. G. Lucas, G. Roghi, M. A. Juncal, C. Hartkopf-Fröder, K. Krainer, and C. Morelli. 2022.

https://doi.org/10.1017/pab.2026.10102 Published online by Cambridge University Press

The Artinskian Warming Event: an Euramerican change in climate and the terrestrial biota during the early Permian. *Earth-Science Reviews* **226**:103922.

Marocchi, M., C. Morelli, V. Mair, U. Klötzli, and G. Bargossi. 2008. Evolution of large silicic magma systems: new U-Pb zircon data on the NW Permian Athesian Volcanic Group (Southern Alps, *Italy).* Journal of Geology **116**: 480–498.

Matamales-Andreu, R., C. F. Kammerer, K. D. Angielczyk, T. R. Simões, E. Mujal, À. Galobart, and J. Fortuny. 2024. Early–middle Permian Mediterranean gorgonopsian suggests an equatorial origin of therapsids. *Nature Communications* **15**:10346.

McGhee Jr, G. R., M. E. Clapham, P. M. Sheehan, D. J. Bottjer, and M. L. Droser. 2013. A new ecological-severity ranking of major Phanerozoic biodiversity crises. *Palaeogeography, Palaeoclimatology, Palaeoecology* **370**: 260–270.

Modesto, S. P., R. M. H. Smith, N. s. E. Campione, and R. R. Reisz. 2011. The last "pelycosaur": a varanopid synapsid from the *Pristerognathus* Assemblage Zone, Middle Permian of South Africa. *Naturwissenschaften* **98**:1027–1034.

Montañez, I. P., and C. J. Poulsen. 2013. The Late Paleozoic ice age: an evolving paradigm. *Annual Review of Earth and Planetary Sciences* **41**:629–656.

Montañez, I. P., N. J. Tabor, D. Niemeier, W. A. Dimichele, T. D. Frank, C. R. Fielding, J. L. Isbell, L. P. Birgenheier, and M. C. Rygel. 2007. CO_2-forced climate and vegetation instability during late Paleozoic deglaciation. *Science* **315**:87–91.

Morelli, C., G. Bargossi, V. Mair, M. Marocchi, and A. Moretti. 2007. The lower Permian volcanics along the Etsch valley from Meran to Auer (Bozen). *Mitteilungen der österreichischen mineralogischen Gesellschaft* **153**:195–218.

Morelli, C., M. Marocchi, A. Moretti, G. M. Bargossi, G. Gasparotto, B. De Waele, U. Klötzli, and V. Mair. 2012. Volcanic stratigraphy and radiometric age constraints at the northern margin of a mega-caldera system: Athesian Volcanic Group (Southern Alps, Italy). *GeoActa* **11**:51–67.

Nicholson, D. B., P. J. Mayhew, and A. J. Ross. 2015. Changes to the fossil record of insects through fifteen years of discovery. *PLoS ONE* **10**:e0128554.

Olson, E. C. 1962. Late Permian terrestrial vertebrates, U.S.A. and U.S.S.R. *Transactions of the American Philosophical Society, new series* **52**:1–224.

Olson, E. C. 1967. Early Permian Vertebrates of Oklahoma. *Oklahoma Geological Survey Circular* **74**:1–111.

Olson, E. C. 1975. Permo-Carboniferous paleoecology and morphotypic series. *American Zoologist* **15**:371–389.

Olson, E. C. 1982. Extinctions of Permian and Triassic nonmarine vertebrates. Pp. 501–511 *in* L. T. Silver and P. H. Schultz, eds. *Geological implications of impacts of large asteroids and comets on the Earth*. Geological Society of America, Boulder, Colo.

Peters, S. E., and M. McClennen. 2016. The Paleobiology Database application programming interface. *Paleobiology* **42**:1–7.

Piñeiro, G., M. Verde, M. Ubilla, and J. Ferigolo. 2003. First basal synapsids ("Pelycosaur") from the Upper Permian-Lower Triassic of Uruguay, South America. *Journal of Paleontology* **77**:389–392.

Poulsen, C. J., D. Pollard, I. P. Montañez, and D. Rowley. 2007. Late Paleozoic tropical climate response to Gondwanan deglaciation. *Geology* **35**:771–774.

Presley, M. W., and K. A. McGillis. 1982. *Coastal evaporite and tidal-flat sediments of the upper Clear Fork and Glorieta Formations, Texas Panhandle*. Report of Investigations no. **115**. Bureau of Economic Geology, Austin, Tex.

Rainford, J. L., and P. J. Mayhew. 2015. Diet evolution and clade richness in Hexapoda: a phylogenetic study of higher taxa. *American Naturalist* **186**: 777–791.

Rampino, M. R., and S.-Z. Shen. 2021. The end-Guadalupian (259.8 Ma) biodiversity crisis: the sixth major mass extinction? *Historical Biology* **33**: 716–722.

Reisz, R. R. 1986. Pelycosauria. Pp. 1–102 *in* P. Wellnhofer, ed. *Encyclopedia of paleoherpetology*. Gustav Fischer, Stuttgart.

Reisz, R. R., and D. S. Berman. 2001. The skull of *Mesenosaurus romeri*, a small varanopseid (Synapsida: Eupelycosauria) from the Upper Permian of the Mezen river basin, northern Russia. *Annals of Carnegie Museum* **70**:113–132.

Reisz, R. R., and M. Laurin. 2001. The reptile *Macroleter*: first vertebrate evidence for correlation of Upper Permian continental strata of North America and Russia. *Geological Society of America Bulletin* **113**:1229–1233.

Reisz, R. R., and M. Laurin. 2002. The reptile *Macroleter*, the first vertebrate evidence for correlation of Upper Permian continental strata of North America and Russia. *Reply*. Geological Society of America Bulletin **114**: 1176–1177.

Reisz, R. R., J. Liu, J.-L. Li, and J. Müller. 2011. A new captorhinid reptile, *Gansurhinus qingtoushanensis*, gen. et sp. nov., from the Permian of China. *Naturwissenschaften* **98**:435–441.

Richey, J. D., I. P. Montañez, Y. Goddéris, C. V. Looy, N. P. Griffis, and W. A. DiMichele. 2020. Influence of temporally varying weatherability on CO_2–climate coupling and ecosystem change in the late Paleozoic. *Climate of the Past* **16**:1759–1775.

Romano, M., N. Brocklehurst, and J. Fröbisch. 2018. The postcranial skeleton of *Ennatosaurus tecton* (Synapsida, Caseidae). *Journal of Systematic Palaeontology* **16**:1097–1122.

Romer, A. S., and L. I. Price. 1940. *Review of the Pelycosauria*. Arno Press, New York.

Rowan, T. H. 1990. *Functional stability analysis of numerical algorithms*. Ph.D. thesis. University of Texas at Austin, Austin.

Ruta, M., and M. J. Benton. 2008. Calibrated diversity, tree topology and the mother of mass extinctions: the lesson of temnospondyls. *Palaeontology* **51**: 1261–1288.

Sahney, S., and M. J. Benton. 2008. Recovery from the most profound mass extinction of all time. *Proceedings of the Royal Society B* **275**:759–765.

Sahney, S., M. J. Benton, and H. J. Falcon-Lang. 2010. Rainforest collapse triggered Carboniferous tetrapod diversification in Euramerica. *Geology* **38**: 1079–1082.

Sato, A. M., E. J. Llambías, M. A. Basei, and C. E. Castro. 2015. Three stages in the Late Paleozoic to Triassic magmatism of southwestern Gondwana, and the relationships with the volcanogenic events in coeval basins. *Journal of South American Earth Sciences* **63**:48–69.

Schneider, J. W., F. Körner, M. Roscher, and U. Kroner. 2006. Permian climate development in the northern peri-Tethys area — The Lodève basin, French Massif Central, compared in a European and global context. *Palaeogeography, Palaeoclimatology, Palaeoecology* **240**:161–183.

Schneider, J. W., S. G. Lucas, F. Scholze, S. Voigt, L. Marchetti, H. Klein, S. Opluštil, R. Werneburg, V. K. Golubev, and J. E. Barrick. 2020. Late Paleozoic–early Mesozoic continental biostratigraphy—links to the Standard Global Chronostratigraphic Scale. *Palaeoworld* **29**:186–238.

Shellnutt, J., G. Bhat, M. Brookfield, and B. M. Jahn. 2011. No link between the Panjal Traps (Kashmir) and the Late Permian mass extinctions. *Geophysical Research Letters* **38**(19).

Sidor, C. A. 2001. Simplification as a trend in synapsid cranial evolution. *Evolution* **55**:1419–1442.

Simões, T. R., C. F. Kammerer, M. W. Caldwell, and S. E. Pierce. 2022. Successive climate crises in the deep past drove the early evolution and radiation of reptiles. *Science Advances* **8**:eabq1898.

Smith, R., B. Rubidge, and M. Van der Walt. 2012. Therapsid biodiversity patterns and paleoenvironments of the Karoo Basin, South Africa. Pp. 30–62 *in* A. Chinsamy-Turan, ed. *Forerunners of mammals: radiation, histology, biology*. Indiana University Press, Bloomington.

Spina, A., L. Marchetti, J. B. Diez, E. Capezzuoli, H. Saleh, I. R. Barreiro, E. Kustatscher, and A. Ronchi. 2026. New palynostratigraphic data from the Kungurian (Cisuralian) Guncina Formation, Athesian District (Southern Alps, northern Italy) with regional-global correlation. *Journal of Iberian Geology* **52**:149–173.

Stanley, S. M. 2016. Estimates of the magnitudes of major marine mass extinctions in earth history. *Proceedings of the National Academy of Sciences USA* **113**:E6325–E6334.

Stanley, S. M., and X. Yang. 1994. A double mass extinction at the end of the Paleozoic Era. *Science* **266**:1340–1344.

Torsvik, T. H., M. A. Smethurst, K. Burke, and B. Steinberger. 2008. Long term stability in deep mantle structure: evidence from the ~ 300 Ma Skagerrak-Centered Large Igneous Province (the SCLIP). *Earth and Planetary Science Letters* **267**:444–452.

Utting, J., and S. G. Lucas. 2010. Palynological investigation of the Upper Pennsylvanian (Carboniferous) El Cobre Canyon Formation, Cutler Group, Canon del Cobre, Rio Arriba County, New Mexico, U.S.A. *New Mexico Museum of Natural History and Science Bulletin* **49**:71–74.

Vallé, F., H. Nowak, E. Kustatscher, S. Erkens, G. Roghi, C. Morelli, K. Krainer, N. Preto, and C. Hartkopf-Fröder. 2023. Reconstructing Kungurian

https://doi.org/10.1017/pab.2026.10102 Published online by Cambridge University Press

(Cisuralian, Permian) terrestrial environments within a megacaldera in the Southern Alps (N-Italy) using lithofacies analysis, palynology and stable carbon isotopes. *Rivista Italiana di Paleontologia e Stratigrafia* **129**:1–24.

Van de Wetering, N., **J. S. Esterle**, **S. D. Golding**, **S. Rodrigues, and A. E. Götz**. 2019. Carbon isotopic evidence for rapid methane clathrate release recorded in coals at the terminus of the Late Palaeozoic Ice Age. *Scientific Reports* **9**:16544.

Viglietti, P. A., **R. B. Benson**, **R. M. Smith**, **J. Botha**, **C. F. Kammerer**, **Z. Skosan**, **E. Butler**, **A. Crean**, **B. Eloff, and S. Kaal**. 2021. Evidence from South Africa for a protracted end-Permian extinction on land. *Proceedings of the National Academy of Sciences USA* **118**:e2017045118.

Wake, D. B., and V. T. Vredenburg. 2008. Are we in the midst of the sixth mass extinction? A view from the world of amphibians. *Proceedings of the National Academy of Sciences USA* **105**(Suppl. 1):11466–11473.

Wang, W.-q., **J. A. Katchinoff**, **C. Garbelli**, **A. Immenhauser**, **Q.-f. Zheng**, **Y.-c. Zhang**, **D.-x. Yuan**, **Y.-k. Shi**, **J. Wang, and N. Planavsky**. 2021. Revisiting the Permian seawater 87Sr/86Sr record: new perspectives from brachiopod proxy data and stochastic oceanic box models. *Earth-Science Reviews* **218**: 103679.

Wang, W.-q., **F. Zhang**, **C.-Y. Liu**, **P. A. P. von Strandmann**, **G. Xiong**, **Q. Zheng**, **C. Garbelli**, **Y. Zhang**, **D. Yuan, and S.-z. Shen**. 2024. Constraints on the continental weathering intensity through the Permian using lithium isotopes of well-preserved brachiopod shells. *Earth and Planetary Science Letters* **648**:119101.

Ward, P. D., **J. Botha**, **R. Buick**, **M. O. De Kock**, **D. H. Erwin**, **G. H. Garrisson**, **J. L. Kirschvink, and R. Smith**. 2005. Abrupt and gradual extinction among late Permian land vertebrates in the Karoo Basin, South Africa. *Science* **307**: 709–714.

Wei, B., **X. Yang**, **X. Cheng**, **M. Domeier**, **H. Wu**, **V. A. Kravchinsky**, **Y. Zhou**, **N. Jiang**, **Y. Wu, and F. Huo**. 2020. An absolute paleogeographic positioning of the early Permian Tarim large igneous province. *Journal of Geophysical Research: Solid Earth* **125**:e2019JB019111.

Willcock, M., **R. A. F. Cas**, **G. Giordano, and C. Morelli**. 2013. The eruption, pyroclastic flow behaviour, and caldera in-filling processes of the extremely large volume (> 1290 km^3), intra-to extra-caldera, Permian Ora (Ignimbrite) Formation, Southern Alps, Italy. *Journal of Volcanology and Geothermal Research* **265**:102–126.

Willcock, M., **G. Bargossi**, **R. Weinberg**, **G. Gasparotto**, **R. Cas**, **G. Giordano, and M. Marocchi**. 2015. A complex magma reservoir system for a large volume intra-to extra-caldera ignimbrite: mineralogical and chemical architecture of the VEI8, *Permian Ora ignimbrite (Italy).* Journal of Volcanology and Geothermal Research **306**:17–40.

Xu, Y.-G., **X. Wei**, **Z.-Y. Luo**, **H.-Q. Liu, and J. Cao**. 2014. The Early Permian Tarim Large Igneous Province: main characteristics and a plume incubation model. *Lithos* **204**:20–35.

Zhang, C., **T. Stadler**, **S. Klopfstein**, **T. A. Heath, and F. Ronquist**. 2016. Total-evidence dating under the fossilized birth–death process. *Systematic Biology* **65**:228–249.

Zhang, Y.-X., and K.-J. Zhang. 2017. Early Permian Qiangtang flood basalts, northern Tibet, China: a mantle plume that disintegrated northern Gondwana? *Gondwana Research* **44**:96–108.

https://doi.org/10.1017/pab.2026.10102 Published online by Cambridge University Press